Title

Using coherence to enhance function in chemical and biophysical systems.

Journal

Nature, 543(7647)

ISSN

0028-0836

Authors

Scholes, Gregory D

Fleming, Graham R

Chen, Lin X

et al.

Publication Date

2017-03-01

DOI

10.1038/nature21425

Peer reviewed

REVIEW

doi:10.1038/nature21425

Using coherence to enhance function in chemical and biophysical systems

Gregory D. Scholes[1], Graham R. Fleming[2], Lin X. Chen[3,4], Alán Aspuru-Guzik[5], Andreas Buchleitner[6], David F. Coker[7], Gregory S. Engel[8], Rienk van Grondelle[9], Akihito Ishizaki[10], David M. Jonas[11], Jeff S. Lundeen[12], James K. McCusker[13], Shaul Mukamel[14], Jennifer P. Ogilvie[15], Alexandra Olaya-Castro[16], Mark A. Ratner[17], Frank C. Spano[18], K. Birgitta Whaley[19,20] & Xiaoyang Zhu[21]

Coherence phenomena arise from interference, or the addition, of wave-like amplitudes with fixed phase differences. Although coherence has been shown to yield transformative ways for improving function, advances have been confined to pristine matter and coherence was considered fragile. However, recent evidence of coherence in chemical and biological systems suggests that the phenomena are robust and can survive in the face of disorder and noise. Here we survey the state of recent discoveries, present viewpoints that suggest that coherence can be used in complex chemical systems, and discuss the role of coherence as a design element in realizing function.

Coherence often hides in complex systems, and its presence is deemed too fleeting to be relevant for robust function. As such, chemists and biologists have not traditionally considered coherence as a powerful tuning element for enhancing or explaining function. But coherence may be misunderstood.

The presence of coherence, and its dominance over an incoherent background, is revealed by a phenomenon known as coherent backscattering. This occurrence is apparent when we view Saturn's rings from Earth. The rings of this celestial body are notably brighter when the Sun is aligned along the direction from Earth to the planet. The principle is that when the light waves enter this disordered medium, they can be scattered precisely in a backward direction. Those precisely backscattered light waves exit the medium so that they line up in step with each other, causing their amplitudes to sum perfectly. As a result, the intensity of this back-scattered light is twice that of light dispersed in other directions[1]. This amplification-like effect is astounding considering the complexity of the scattering process, through the millions of randomly arranged ice crystals that comprise Saturn's rings, and then returning along the same path. Adding wave amplitudes in phase is a more powerful concept than would be anticipated, and gives rise to the notion of harnessing coherence as an element of design.

Coherent backscattering can be seen on much smaller spatial scales too, such as when it is used to improve light absorption in solar cells[2] or when the effect enables lasing in disordered media such as plastic or powdered semiconductors[3,4]. Likewise, scattering in periodic structures leads to 'localized light', which is made use of in photonic crystals, suggesting a way to control light transmission[5]. Other kinds of correlations produce striking enhancement of interactions between nanoscale systems. For example, when charge density fluctuations are correlated over long length scales, exceptional long-range van der Waals forces result[6]. Such attractive forces are impossible to attain by an incoherent sum of interactions from local fluctuations along the breadth of the materials.

We are accustomed to viewing functional biological systems as operating classically, so when quantum coherence appears, it seems surprising. However, recent discoveries of coherence phenomena in various biological and materials systems[7–11] suggest the viability of coherence-enhanced function. In addition, coherence has been widely discussed as a means of improving transport in disordered and complex systems[12]. Examples include long-range transfer of electronic excitation—light harvesting—in photosynthesis and efficient, almost unidirectional charge separation at donor–acceptor interfaces in organic photovoltaics. While it is stimulating to consider unique microscopic protocols for employing coherence and quantum effects, greater inspiration lies in leveraging these effects to yield ways of optimizing materials, energy transduction and multi-molecular machines, or to devise potent routes for chemical syntheses.

Here we evaluate opportunities to harness electronic and nuclear coherences to realize energy transduction or chemical transformation including, but not limited to, reactions driven by light. We examine current examples that indicate how function has been enhanced by engineering dynamics in a coherent regime. We explore the way coherence can change the way we approach designing for function. We build our discussion around examples from the literature, but we do not attempt to review the full scope of work that has been published in the past few years.

Defining and detecting coherence

Coherence can be classical or quantum mechanical and comes from well defined phase and amplitude relations where correlations are preserved over separations in space or time. Whereas for classical coherence we intuitively expect to detect a recurring pattern, quantum mechanical

[1]Department of Chemistry, Princeton University, Princeton, New Jersey 08544, USA. [2]Department of Chemistry, University of California, Berkeley and Molecular Biophysics and Integrated Bioimaging Division, Lawrence Berkeley National Laboratory, Berkeley, California 94720, USA. [3]Chemical Sciences and Engineering Division, Argonne National Laboratory, Lemont, Illinois 60439, USA. [4]Department of Chemistry, Northwestern University, Evanston, Illinois 60208, USA. [5]Department of Chemistry and Chemical Biology, Harvard University, Cambridge, Massachusetts 02138, USA. [6]Institute of Physics, Albert-Ludwigs-Universitaet Freiburg, D-79104 Freiburg, Germany. [7]Department of Chemistry, Boston University, Boston, Massachusetts 02215, USA. [8]Department of Chemistry, University of Chicago, Chicago, Illinois 60637, USA. [9]Department of Physics and Astronomy, VU University Amsterdam, 1081HV Amsterdam, The Netherlands. [10]Institute for Molecular Science, National Institutes of Natural Sciences, Myodaiji, Okazaki 444-8585, Japan. [11]Department of Chemistry and Biochemistry, University of Colorado Boulder, Boulder, Colorado 80309, USA. [12]Department of Physics, University of Ottawa, Ottawa, Ontario K1N 6N5, Canada. [13]Department of Chemistry, Michigan State University, East Lansing, Michigan 48824, USA. [14]Departments of Chemistry and Physics and Astronomy, University of California—Irvine, Irvine, California 92697, USA. [15]Department of Physics, University of Michigan, Ann Arbor, Michigan 48109, USA. [16]Department of Physics and Astronomy, University College London, London WC1E 6BT, UK. [17]Department of Chemistry, Northwestern University, Evanston, Illinois 60208, USA. [18]Department of Chemistry, Temple University, Philadelphia, Pennsylvania 19122, USA. [19]Department of Chemistry, University of California—Berkeley, California 94720, USA. [20]Chemical Sciences Division, Lawrence Berkeley National Laboratory, Berkeley, California 94720, USA. [21]Department of Chemistry, Columbia University, New York, New York 10027, USA.

BOX 1

Quantum mechanical coherence and decoherence

Chemists are familiar with the concept and importance of quantum mechanical coherence in the context of magnetic resonance. In that case coherence means that spins are superposition states—wavefunctions of the form $\psi_i = c_\uparrow|\uparrow\rangle \pm c_\downarrow|\downarrow\rangle$, manifest as net spin polarization perpendicular to the magnetic field. Usually ensembles of (non-interacting) spins are observed in an experiment, and can be thought of as a collection of independent spins with individual coherences (provided the spins are considered to be distinguishable) between their orientations $|\uparrow\rangle$ and $|\downarrow\rangle$.

The full information on the system is encoded in the associated statistical operator or density matrix. Since nothing more is to be known about the quantum state of the spin, the density matrix (note this is an ensemble average) is directly associated with the system state and itself often simply called the 'state'. Probabilities of finding populations of a spin state are indicated in diagonal elements of this matrix, $|\uparrow\rangle\langle\uparrow|$ and $|\downarrow\rangle\langle\downarrow|$. However, this matrix encodes considerably more information than just the probabilities, namely coherences. Coherences are indicated by the 'off-diagonal' values, which in this example include $|\uparrow\rangle\langle\downarrow|$ and $|\downarrow\rangle\langle\uparrow|$. Note that coherence is a property of a state and it is dependent on the choice of basis because it is defined with respect to a certain basis (here the spin basis comprising $|\uparrow\rangle$ and $|\downarrow\rangle$). Other kinds of measures that do not depend on the representation basis can be used to analyse the coherence properties of a given state, such as the 'purity'—defined as the trace of the square of the density matrix.

Coherence will generally diminish with time following its creation by, for example, an ultrashort light pulse. The loss of coherence is referred to as decoherence or dephasing, and although these terms mean different things they are often used interchangeably. Decoherence may be understood as a purely quantum mechanical phenomenon that arises from the observed system becoming quantum mechanically entangled with the unobserved bath (environment) degrees of freedom. Averaging over the latter leads to an irreversible decay of the off-diagonal elements of the density matrix of the system; this decay can also be induced by classical noise. The system thus irrevocably loses its ability to exhibit interference phenomena. Dephasing, on the other hand, has contributions from both decoherence and from an ensemble effect that arises because different ensemble members evolve slightly differently, so that phase correlations across the ensemble are progressively reduced on average, even though the coherence may be much longer-lived in each individual member of the ensemble. Even after complete dephasing, phase correlations and the ability to display interference can then often be resurrected by spin-echo-like experiments. We usually understand dephasing to come from a statistical average over an environment comprising many degrees of freedom that couples to the system but which cannot be observed directly. In the context of chemistry, the bath is the solvent—physically all the solvent molecules jiggling around randomly and coupled to the system (a solute) by solvation forces.

coherence is exemplified by superposition states. The distinction between classical and quantum coherence is not always obvious, but is indicated by special correlations—a notable example is photon bunching and anti-bunching[13]. Quantum superposition states have properties that are not realized in classical superpositions[14].

We are probably more familiar with quantum mechanical coherence than we realize. For example, chemists know there are two ways of drawing the alternating double and single bonds in a benzene ring and that these two structures, φ_1 and φ_2, are in 'resonance', meaning that, from the perspective of classical valence bond theory[15], the electronic ground state is a quantum mechanical superposition state that includes resonance of these Kekulé structures: $c\varphi_1 + c\varphi_2 + \cdots$. More limited delocalization can mix the wavefunctions of an electron donor and acceptor into an intervening bonding bridge. When this occurs, the bonding bridge enables remarkably long-range electron transfer (20–30 Å) reactions through chemical bonds in supramolecular systems, or through proteins to instigate biological redox chemistry[16–18].

Coherence effects that result from strong resonance interactions are robust and decisive in their roles for function because these states are little perturbed by disorder and fluctuating interactions. Other coherences are fragile, as it is difficult to maintain states in lock-step when the system is subject to strong random fluctuations—this process in which phase coherence is lost is called decoherence. Coherence and decoherence are, therefore, competing processes; see Box 1. To understand conceptually how energy gap fluctuations affect resonances and, upon appropriate averaging, give rise to decoherence, the example of "flickering resonance" can be helpful[19].

Adding wave amplitudes, or interference phenomena, has dramatic consequences. For example, when a molecule spans two electrodes[20,21] transport junctions form, revealing striking differences in current according to the interference of the pathways by which electrons can be routed through a molecule[22,23]. As the electron tunnels through the molecule it traverses physical, structural pathways according to the amplitudes and energies of molecular orbitals[24–26]. Quantum interference between pathways through the π-system can prevail, despite competing pathways through the σ-bonds. We illustrate in Fig. 1a and b representative calculations from this rich field of investigation. We show two contrasting cases of tunnelling through di(thioethyne)benzene molecules—the electron tunnels from one electrode through the benzene ring to the other electrode, via the input and output thioethyne linkers. Linkers can be positioned at different relative positions on the sixfold symmetric benzene ring. In the *para*-linked molecule, the two principal pathways are identical and, therefore, interfere constructively and ensure high transmission. In contrast, *meta*-linking the two thioethyne groups in the same chemical moiety results in the electron traversing two different pathways around the aromatic ring. Destructive interferences result and

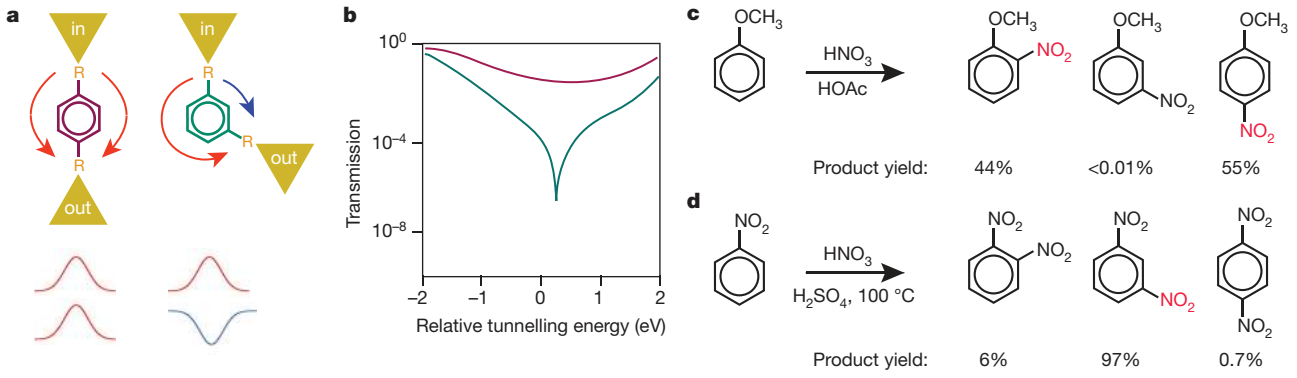

Figure 1 | Coherence phenomena. a, Conceptual illustration of the electron wavefunction amplitude for two alternative transmission paths through the molecule. R = thianoethyne. The gold triangles represent the electrical contacts of the molecular transport junction apparatus. **b**, Current transmission curves predicted for the *para*-configuration molecule (red) and the *meta*-configuration molecule[24] (green). **c**, **d**, Examples of prototypical electrophilic aromatic substitution reactions.

BOX 2

Two-dimensional electronic spectroscopy

The information content of the simplest absorptive 2D spectra can be appreciated by considering an experiment in which a tunable laser excites the sample and changes in its absorbance spectrum are measured for all detection frequencies as a function of the tunable excitation frequency. Like a topographic map, the 2D spectrum shows contours indicating the decrease in absorbance as a function of the excitation and detection frequencies. In the example in Box 2 Figure, the sample with the linear absorbance spectrum shown on the left has four peaks that could arise from four molecules with one peak each, one molecule with four peaks, or any intermediate combination. The 2D spectrum shown has eight peaks: four diagonal peaks with $\omega_{excitation} = \omega_{detection}$ plus four off-diagonal 'cross-peaks'. To understand this 2D spectrum, consider the 2D spectrum of the molecule α with energy level structure defined by the spectrum shown on the left in blue. The sample will be unaffected for $\omega_{excitation} < \omega_a$, so the 2D spectrum shows no change in absorbance. However, when $\omega_{excitation} = \omega_a$, some α molecules are transferred out of their ground state and into their first excited state. Because this decreases the concentration of α molecules in the ground state, the Beer's law absorbance decreases for every transition starting in the ground state of α, generating 2D peaks at $\omega_{detection} = \omega_a$ and $\omega_{detection} = \omega_c$. The diagonal 2D peak at (ω_a, ω_a) is stronger than the cross-peak because of stimulated emission from the population transferred to the first excited state, which further decreases the absorbance change detected at ω_a, but not at ω_c (since no molecules were transferred to the second excited state by excitation at ω_a). As the tunable laser frequency is increased, nothing happens to α until α is excited to its second excited state at $\omega_{excitation} = \omega_c$. The decrease in Beer's law absorbance again generates 2D peaks at $\omega_{detection} = \omega_a$ and $\omega_{detection} = \omega_c$, and this time the diagonal 2D peak at (ω_c, ω_c) is stronger because of stimulated emission. The 2D spectrum of β can be understood in the same way as that of α. Because β molecules are completely unaffected by excitation of α, and vice versa, the 2D spectrum of their mixture is the sum of the 2D spectra of the individual components. The presence and absence of 2D cross-peaks are equally informative: the presence of 2D cross-peaks at (ω_a, ω_c) and (ω_c, ω_a) proves that the peaks at ω_a and ω_c in the linear absorption spectrum come from the same molecule; the absence of cross-peaks at (ω_a, ω_b) and (ω_b, ω_a) proves that the peaks at ω_a and ω_b in the linear absorption spectrum come from different molecules. Thus, the 2D spectrum directly separates the linear absorbance spectrum of the mixture on the left into the spectra of its components on the right. In general, 2D spectra are more complicated than this simple example, which neglects the possibility of absorption transitions originating from the excited states.

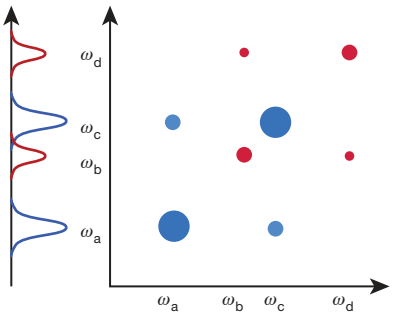

Box 2 Figure | How to read a 2D spectrum.

are evident in the transmission spectrum as markedly suppressed transmissions at various energy resonances. These observations contrast with predictions from circuit analogues where resistors are wired in parallel[23].

A similar partitioning of *ortho*/*para* versus *meta* pathways is well known in synthetic chemistry, and is widely exploited in electrophilic aromatic substitution reactions. The withdrawal or addition of electron density by a substituent defines a particular pattern of electron density at the *ortho*, *meta* and *para* positions and primes them for directed attack by the reagent. In this case, electron-donating reagents yield *ortho* or *para* substitution, while electron-withdrawing reagents direct *meta* substitution; see Fig. 1c, d. This serves to show how quantum interference might have wider implications, but we note that there is a broad literature on aromatic C–H activation chemistry that does not easily connect with the elegant explanations of single-molecule conductance.

In many systems, such as complex molecules or even single electrons or photons, coherence can be difficult to measure. Standard measurements tend to hide coherence because they measure only probabilities—that is, the diagonal elements of the density matrix—either in a particular basis that is unique to the experiment or in a basis that changes with time, for instance as excitons localize. Despite this challenge, it is important to assess coherence in order to obtain feedback on design principles. Function comes from dynamics, a transformation from reactants to products, and optimal microscopic dynamics results from a balance between coherence and dissipation. Between the limits of this interplay, there must be a maximum in the rate[27].

Coherence can be detected reasonably easily using specialized measurements. For example, short laser pulses can excite ladders of states in phase, thereby making a superposition that can be detected using two-dimensional spectroscopy; see Box 2. A cross-peak in the 2D map labels the excited and detected transitions (Box 2 Figure), while oscillations in the cross-peaks as a function of pump–probe waiting time reveal coherences involving those transitions marching together in time. This does not last forever—the oscillations damp away as a function of waiting time as a consequence of dephasing, giving a lower bound for the decoherence time of the quantum superposition. An example of electronic coherence is shown in Fig. 2a–c. Broad-band femtosecond pulses overlap the first two exciton states, heavy-hole exciton (HX) and light-hole exciton (LX), of a semiconductor 'nanoplatelet' colloid dispersed in ambient-temperature solution[28]. The amplitude of the cross-peaks, HX-LX and LX-HX, in the 2D signal map oscillate as a function of excitation-detection time delay, showing that the amplitude of HX and LX bands indeed are correlated until the superposition dephases. The dephasing of this ensemble happens with a time constant of 13 fs. Electronic coherences at ambient temperature typically decohere with a time constant of $\leq$100 fs.

Similarly, vibrational ladders in molecules can be impulsively excited as superposition states (vibrational coherences) by short laser pulses; see Fig. 2d, e. In Fig. 2d the transient absorption spectrum of a chromophore cresyl violet in solution as a function of the pump–probe time delay is shown. Notice the ripples on top of the spectrum—these indicate the in-step phase of the vibrational coherence synchronously swinging backwards and forwards in the vibrational potential of each mode[29]. The coherences are better revealed by removing the slowly changing signal amplitude due to population kinetics; see Fig. 2e. Vibrational coherences typically decay with time constants in the picosecond range.

An outstanding challenge is to relate the detected coherence to its role in function, and this goal probably requires more detailed characterization of wavefunction amplitudes and phases. The challenge comes down to how to reconstruct essential features of a wavefunction by a series of measurements of observables. For example, even for a simple light wave, four carefully referenced unique measurements of the transmitted intensity of a light beam through various polarizers and waveplates are needed to measure the polarization state[30]. That inspires a strategy for characterizing quantum superpositions[31]. Clearly new kinds of characterization tools for complex molecular systems are essential. Recently, it has been demonstrated that a technique known as weak measurement allows for direct access to the wavefunction[32] or density matrix of a system[33]. In a weak measurement the system is only very weakly perturbed in each measurement trial and a correspondingly small amount of information about its state is learned. Averaging over repeated measurements on an ensemble allows the density matrix to be pieced together. Monitoring biological and chemical systems by weak measurements thus offers a new way to study the role of coherence in their function; see Box 3.

Vibronic coherence

As molecules are complex, their spectroscopy is often not well described as a simple ladder of states. Instead, the interplay among electronic and nuclear motions can lead to quite complicated vibronic levels and mixing between electronic and vibrational wavefunctions[34–37]. This mixing is

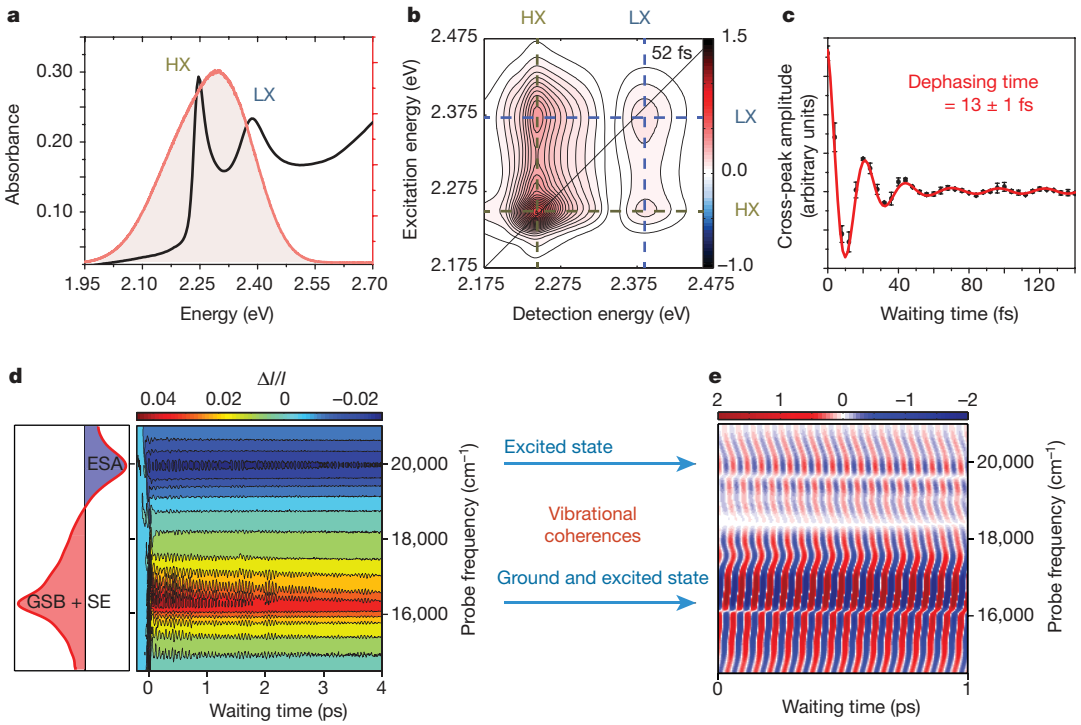

Figure 2 | Coherences revealed by experiment. a, Absorption spectra of CdSe nanoplatelets (black line) showing the HX and LX exciton transitions. The spectrum of the laser pulses used in the 2D spectroscopy experiments is shaded orange. **b**, 2D electronic spectrum recorded at a pump–probe delay time of 52 fs. **c**, Amplitude oscillations in the lower cross-peak of the rephasing 2D spectrum for a CdSe/CdZnS nanoplatelet (the real part with population relaxation subtracted) as a function of the waiting time. Error bars, s.d. estimated from three different measurements. Images in **a**–**c** adapted from ref. 28, Nature Publishing Group. **d**, A contour map of broadband pump–probe data for cresyl violet solution, showing the oscillatory modulation on top of ground- and excited-state population dynamics. The data are recorded as the change in probe transmission after the pump pulse (ΔI), normalized by the transmission without the pump (I). ESA, excited-state absorption; GSB, ground-state bleach; SE, stimulated emission. Image adapted from ref. 106, American Chemical Society. **e**, Fourier-filtered pump–probe data revealing coherent oscillations of the strong Franck–Condon active modes.

important for understanding spectroscopy, intramolecular dynamics and chemical reactions[35], and it changes the intuitive translation from spectroscopy to dynamics. Simulations and experiments are needed to identify electronic and vibrational coherence, and combinations known as vibronic coherence in which it is impossible to otherwise discriminate electronic from vibrational energy ladders.

A range of phenomena result, collectively called vibronic coupling. Delocalization via vibronic coupling can be robust to environmental fluctuations and it provides an opportunity for chemical design because the underlying vibrational resonances are readily be tuned by structure. The recognition of functional vibronic coherence in biological and chemical systems has been inspired by the discovery and subsequent investigation of surprising coherent oscillations revealed by 2D electronic spectroscopic studies of photosynthetic systems[7,9,10]; see Fig. 3a, b.

To illustrate how interaction between molecules changes an intuitive ladder of vibrational levels into a more complicated set of states, model calculations of two interacting molecules[35] (electronic coupling 50 cm^{-1}, energy gap 650 cm^{-1} and vibrational frequency of 600 cm^{-1}) are plotted

BOX 3

Measuring and assessing coherence

Although coherence is theoretically well defined and also accessible to experimental quantification, it is more difficult to ponder the role of the coherence detected in a dynamically evolving reaction or transport process than in stochastic activation and transfer processes. Often dynamical coherence can prevail only on shorter scales. We then need to understand how coherence on these short scales can condition functionality on large scales. In such a scenario we would like to monitor the interplay of coherent and incoherent processes in real time, without disrupting their progress. However, given the intricate structure and the complexity of interactions between molecules and the environment, considerable conceptual and experimental advances are needed to achieve this. The technique of weak measurement allows direct access to the density matrix or state of a quantum system, without much perturbing it. A challenge is to port this method, so far employed only in quantum optical contexts, to truly complex molecular assemblies.

In weak measurement two quantum systems are weakly coupled by some interaction. This interaction is typically used to model how measurement generally works (hence the term 'weak measurement'). That is, one system is considered the system under study and the other the measurement apparatus[107]. In practice, often these two systems are actually just two different degrees of freedom of the same system, for example, the spin and position of an electron.

If the coupling were strong, the two systems would become strongly correlated (in fact, entangled). For example, the indicator reading on the measurement apparatus would correlate exactly and unambiguously with the value of the measured parameter in the system under study. If one observes the indicator, it will collapse to a particular reading and the system under study will collapse the corresponding basis state. On the other hand, if the coupling is weak, the two systems are imperfectly correlated; each distinct indicator reading now corresponds to many states of the system under study. In this case, although an observation of the indicator would give ambiguous results, this ambiguity is precisely what maintains the superposition of states in the system under study, thereby avoiding collapse. And, remember, collapse in a particular basis destroys coherence between the basis states. A small amount of the coherence of the system under study is transferred to the measurement apparatus. Thus, by averaging over many trials and performing a tomographic reconstruction, one can in many cases extract the real and imaginary parts of the full density matrix.

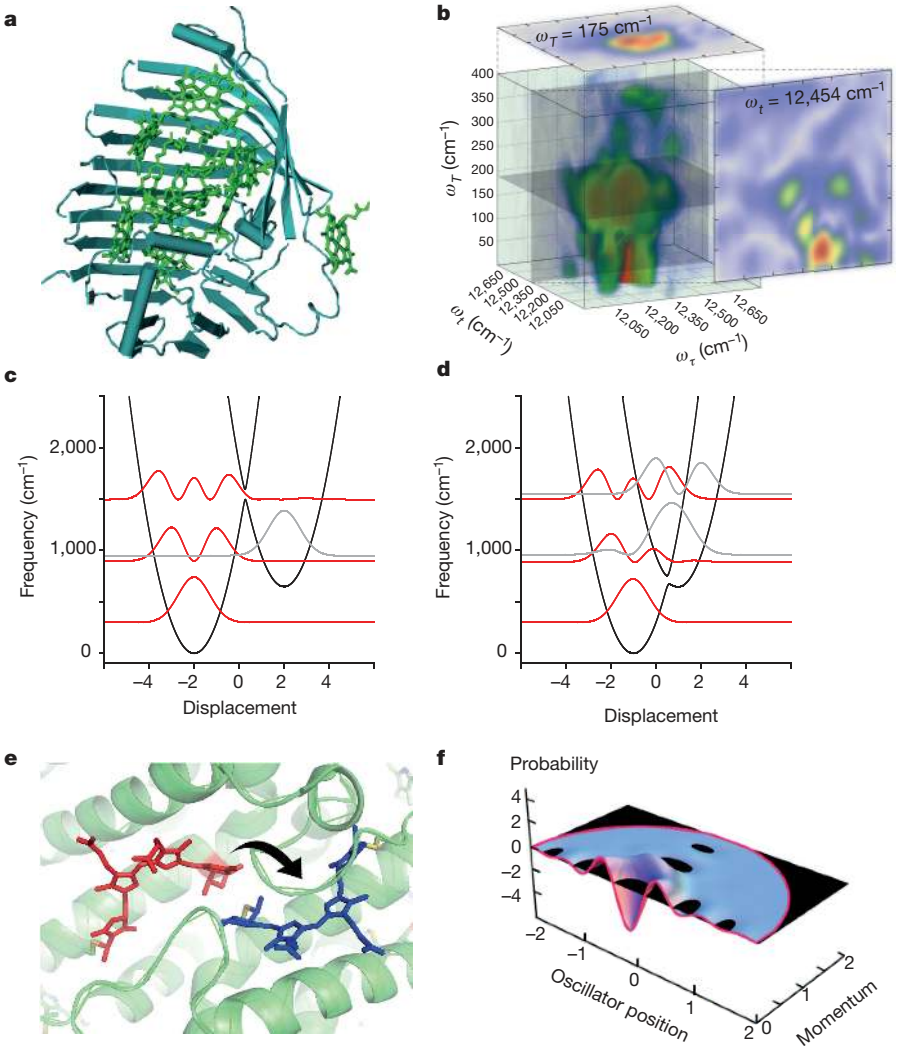

Figure 3 | Vibrations change the picture. a, Structural model of the FMO complex from a green sulfur bacterium. The eight resolved chromophores are indicated. **b**, Quantum beating signatures for a 77 K FMO 2D spectrum, with axes ω_τ and ω_t Fourier transformed with respect the waiting time T, show the frequencies ω_T associated with the energy differences among the excitons. Image reproduced from ref. 76, Elsevier. **c**, Vibronic wavefunctions of two weakly interacting molecules, plotted in red (grey) for vibronic states that are localized mostly on the left (right) molecule. The black curves are the crude adiabatic potentials. These results show that excitations are independently localized on each molecule (electronic coupling 50 cm^{-1}, mode frequency 600 cm^{-1}, energy gap 650 cm^{-1}, dimensionless displacement 4.0). **d**, As coupling to vibrations becomes weaker (dimensionless displacement, 2.0), the vibronic densities delocalize across the two molecules. **e**, Model dimer of bilin molecules from the light-harvesting complex PE545, where excitonic states are quasi-localized. **f**, Regularized Glauber–Sudarshan probability distribution, which is a phase-space distribution used to write the density matrix of the state of the vibrations in the basis of coherent states. Rather than true probability, negative values make this a quasi-probability distribution in phase space. Such negative values cannot be exhibited by the state of any classical system, and are thus unambiguous signatures of the quantum character of the state[45].

in Fig. 3c, d. When the vibrational reorganization energy is large (Fig. 3c) it is clear that the spectroscopy is a simple sum of those of the individual molecules. When the displacement is smaller (Fig. 3d) the vibronic transitions become delocalized across the two molecules. This is the case where exciton–vibration delocalization is amplified by resonance between the excitonic gap(s) and vibrational frequencies[38]. Physically, the displacement represents a change in geometry of the molecule along each normal mode upon photo-excitation, as equilibrium geometries are different in each electronic state.

Vibronic transitions are crucial for enhancing energy transfer rates, as evident in the Förster spectral overlap, because they provide many combinations of energy differences. Similarly, vibronic states provide a manifold of donor and acceptor states that can bridge large free-energy differences and increase rates of electron transfer immensely[39].

Recent work has examined the implications of these delocalized vibronic states for 2D spectroscopy and light-harvesting mechanisms[38,40–43]. It has been proposed that discrete vibrational modes of electronically coupled chromophores may generate and regenerate coherence against a background of dephasing if the exciton–vibration coupling is sufficiently strong[44]. Other work suggested that coherent vibronic energy transfer has signatures of quantum mechanical probability laws[45]; see Fig. 3e, f. In this case, when analysing the collective nuclear motions coupled to the excited state dynamics, it was found that the distribution of the occupation number of the vibrational motion driving energy transfer between molecules is much narrower than predicted for a classical coherent system. Such small fluctuations can only be described by quantum phase-space quasi-probability distributions that have negative values (Fig. 3f), which is a feature impossible to find in a classical system. Experimental approaches that certify the non-classical nature of coherence in chemical and biophysical systems are essential if we are to understand what functionalities can be enhanced or achieved only via quantum coherence.

Studies of other systems ranging from organic photovoltaics to photosynthetic reaction centres associated with the oxygen-evolving complex

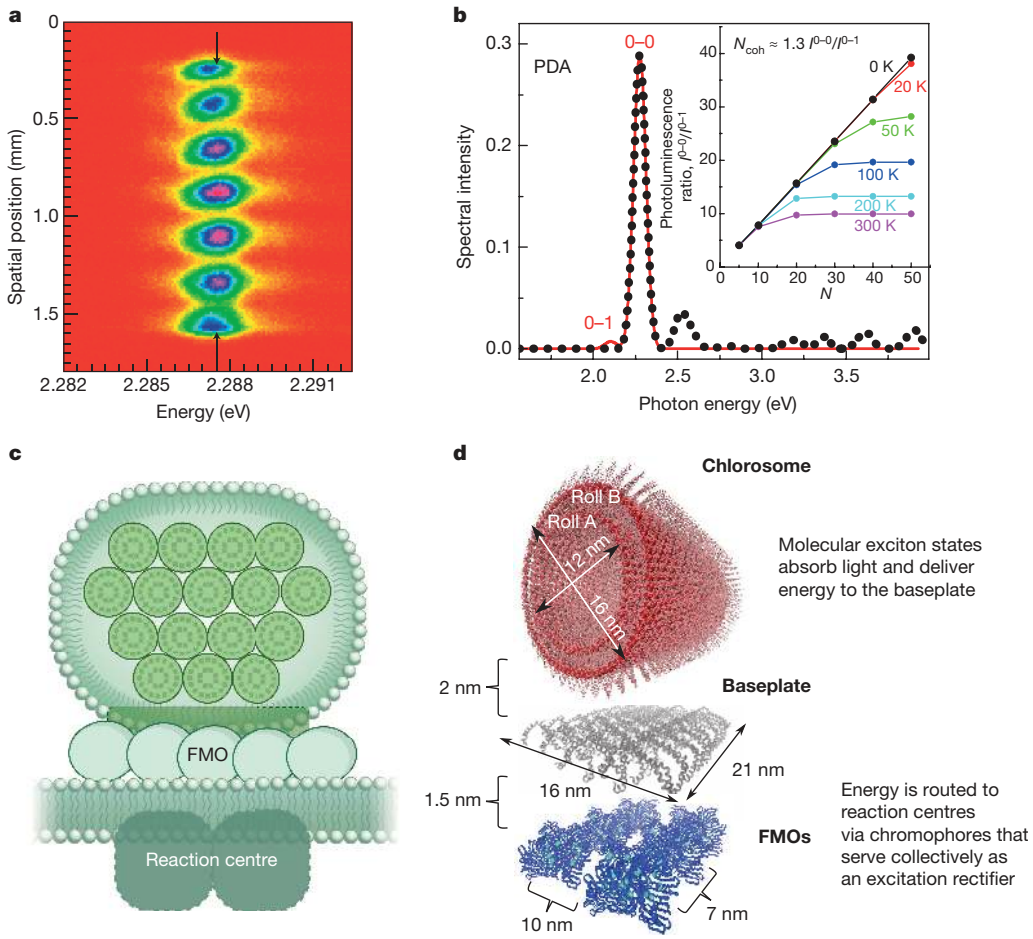

Figure 4 | Long-range excitons. a, Fluorescence interference pattern obtained from two 1-μm-wide emitting regions of a 10-μm-long chain of polydiacetylene (PDA), suggesting an extraordinary coherence length for the exciton. Image reproduced from ref. 52, Nature Publishing Group. **b**, Absorption spectra (black dots) and photoluminescence emission spectra (red line) predicted for polydiacetylene chains chains with $N = 50$ repeat units at $T = 0$ K calculated numerically using the multiparticle basis set[50]. The inset shows how the calculated photoluminescence ratio $I^{0\text{-}0}/I^{0\text{-}1}$ depends on N for various temperatures. The linear behaviour at low temperatures saturates at higher temperatures, indicative of a convergent coherence number, with $N_{coh} < N$. **c**, Illustration of the chlorosome light harvesting complex and associated proteins that transport excitation energy to the reaction centre in green sulfur bacteria. Light is absorbed by the chlorosome, which consists of cylindrical molecular aggregates (top), and is transferred to the FMO complexes via the intermediate 'baseplate'. Excitation subsequently flows to the reaction centres. **d**, The atomistic model used for simulations. It includes the chlorosome (red), baseplate (grey) and FMO complexes (blue). Image adapted from ref. 67, American Chemical Society.

photosystem II (PSII) have revealed notable coherent oscillations using ultrafast spectroscopy[46–48]. Many of these oscillations have frequencies of vibrational modes identified in resonance Raman and fluorescence line-narrowing spectra, and some of these frequencies also match frequency differences between the exciton states. The key result in the case of PSII is that resonance between excitons and vibrational levels in charge-transfer states leads to vibronic mixing that is hypothesized to optimize the flow of population to the terminal charge-separated state[49].

As well as modifying spectral band progressions, vibronic coupling can localize excitation or charge. The manifestation of vibronic coupling in spectra of molecular aggregates can therefore be used to measure exciton delocalization by relating the mean delocalization length of excitons to the ratio of the electronic photoluminescence band intensity (I^{0-0}) and the first vibronic band (I^{0-1})[50,51]. Analysis of the photoluminescence ratio reveals the extraordinary coherent delocalization of the exciton along disorder-free polydiacetyelene chains[50,52] (Fig. 4), estimated to be 30–50 nm at 15 K.

Coherent excitons are prevalent and robust

Coherence is certainly used in photosynthetic light harvesting[53], as evidenced by strong electronic coupling that delocalizes excitation to produce new effective chromophores that span multiple molecules. These effective light-absorbing states are known as molecular excitons[54]. Delocalization in molecular exciton states is a kind of coherence that is robust to dephasing between excitons because energy fluctuations at individual molecular sites are averaged away[55]—that effect is observed as narrow spectral line shapes. Molecular excitons can have substantial functional implications for materials[56].

Light is absorbed and emitted collectively by these delocalized states, and the interplay of phases in the light-absorbing units that decide the properties of molecular excitons can be effectively modelled by scattering of standing waves[57], emphasizing how the excitonic optical properties derive from coherence. Energetic disorder disrupts these perfect wave-like properties underpinning exciton states, thereby diminishing their delocalization through space[12,58]. Delocalization competing with localization is seen in experimental data and is well illustrated by recent studies of various supramolecular systems[59–61] as well as in natural ring-shaped light-harvesting complexes from purple bacteria[62]. Superradiance is the collective fluorescence emission from two or more interacting chromophores, which lead to shorter radiative rates (analogously to coherent backscattering). Superradiant enhancement of emission reveals the robustness of exciton delocalization[63].

Exciton states strongly affect light harvesting because the energy donor and/or acceptor are not single molecules, like the case treated in normal

Förster theory. Instead, the energy donor and/or acceptor comprise the exciton states shared between strongly interacting chromophores. New effective chromophores for light harvesting can thus be constructed, or in nature they can evolve based on pigments already employed by a photosynthetic organism—amply demonstrated by the B850 ring in the LH2 light-harvesting complex of purple bacteria[64]. A modified version of Förster theory accounts for the way these non-additive effects in excitonic donors and acceptors promote energy transfer, and we call this the Generalized Förster Theory (GFT)[64–66].

In GFT, the donor and/or acceptor states are delocalized—this is strong electronic coherence—but owing to a separation of timescales (energy scales of electronic couplings) the energy transfer from donor to acceptor is treated as incoherent, just as in Förster theory. Keeping in mind the interplay between delocalization and decoherence (Box 1), states can be much more delocalized when serving as excitation acceptors than donors. The delocalization of excitation within donor and/or acceptor manifolds enables remarkable acceleration of the energy transfer rate because the collective transition dipoles are much larger than molecular transition dipoles. Also, in marked contrast to Förster theory, dark exciton states are often similarly good excitation donors or acceptors because of how the dipole approximation fails to account for the structure of molecular aggregates[64]. For B800 to B850 energy transfer in LH2, the rate is predicted to be ten times faster than the simulations that assume excitation is localized on bacteriochlorophyll molecules[65]. A similar example of how delocalization can enhance energy transfer is found in the chlorosome antenna complex of green sulfur bacteria[67]; see Fig. 4c, d.

The complexity of theory needed to predict energy transfer depends on a balance of frequency scales, as discussed in section 'Defining and detecting coherence', necessitating development of sophisticated theories to describe details of the energy-transfer mechanism[68–72]. What evidence is there that these complicated theories are necessary? To establish this, we need to develop experiments that record not only rates of energy transfer, but also provide insight into the mechanism and provide stronger tests for theoretical models. Two-dimensional (2D) electronic spectroscopy[73–75] has enabled such experiments. For example, long-lived coherent oscillations—whatever their precise origins—observed in 2D electronic spectra of the Fenna–Matthews–Olson (FMO) complex (Fig. 3a, b) as a function of pump–probe waiting time[76], challenge the predictive power of theories for assessing the competition, or cooperation, of coherent and incoherent reaction mechanisms[7,10].

Coherent charge transport

In the sense of long-range periodic electronic states (Bloch functions), coherence is the basis for describing charge transport in crystalline solids. In such solid-state systems, decoherence can be caused by phonons, collective vibrations of the lattice that include vibrations that couple to optical transitions. When electron–phonon coupling is much weaker than electron–electron interactions, as is the case for most crystalline inorganic semiconductors and metals, an electronic wavefunction is delocalized over the extended lattice and is well described in momentum space by the single-particle band structure. Coherent movement of a low-energy electron or hole can be described by ballistic motion of a free electron or hole with effective mass determined by the band curvature near the conduction-band minimum or valence-band maximum. Scattering by phonons and charged defects disrupts the coherent motion of these carriers, leading to diffusive transport when the scattering is strong.

The discovery of highly efficient solar cells from hybrid organic–inorganic perovskites (HOIPs) has triggered accelerated research in this field[77]. HOIPs are easily formed from solution at ambient temperature and therefore should contain a high density of structural defects. Surprisingly, photophysical and transport measurements reveal the behaviour expected for intrinsic and defect-free semiconductors[78], including long-lived charge carriers with lifetimes more than three orders of magnitude longer than those in conventional semiconductors, suggesting drastically reduced electron–phonon scattering rates[79]. The exceptional properties of HOIPs are hypothesized to arise from coherent transport of carriers and the way carriers couple to lattice vibrations to form polarons. The size difference between polarons results in markedly different transport properties[79,80]. A large polaron moves coherently and its mobility depends inversely on temperature. The large polaron may provide the protection mechanisms essential to shield charge carriers from each other and from charged defects[81].

Is coherent charge transport important in disordered molecular systems? This is a question that has been examined in the context of conjugated materials for solar energy conversion[56] and charge transport along DNA strands[82].

Transition-metal complexes

From biochemistry to catalysis (both thermal and photochemical) to solar energy conversion, transition-metal complexes have important roles. Their relevance comes about owing to the interdependent electronic and structural features that arise from the involvement of *d* orbitals in the valence configurations of such compounds. The Jahn–Teller distortion—ubiquitous in transition metal complexes—is closely related to the vibronic exciton model discussed above[83]. For instance, the D_{2d} symmetric bis(diimine)copper(I) complex flattens to D_2 symmetry upon photoexcitation. The sequence of motions involved has been followed in experiments detecting coherent vibrational wavepackets[84]; see Fig. 5a. It was found that the b_1 symmetry 290 cm^{-1} vibration decoheres as its vibrational energy flows to the low-frequency b_1 flattening mode and the molecule changes shape.

Structural motion can drive coherent changes to electronic structure when it modulates metal–metal interactions. For example, the di-Pt(II) complex, $[Pt(ppy)(\mu\text{-}t\text{-}Bu_2pz)]_2$ (where ppy is 2-phenylpyridine and t-Bu_2pz is 3,5-di-*tert*-butylpyrazolate), undergoes a metal-to-ligand charge-transfer transition upon photoexcitation and, subsequently, the Pt–Pt equilibrium distance contracts. For this reason, electronic coupling between the two halves of the molecule is modulated by metal–metal vibrational motion[85]; see Fig. 5b.

Persistent coherence through an electronic state change is observed in studies of chromium acetylacetonate[86], where excitation into the lowest-energy spin-allowed ligand-field absorption of this compound results in rapid intersystem crossing from a quartet to doublet spin excited state in <100 fs. Coherent oscillations produced by excitation of the initial quartet state do not decohere during the radiationless transition; see Fig. 5c. Studying these coherent motions in the context of wavepacket dynamics may suggest ways to reengineer molecules so as to manipulate the excited-state dynamics.

Function from coherence

While coherence comes in many forms and modifies dynamics in different ways, it often involves complex correlations and might be hidden from the experimenter. Regardless, exploiting coherence clearly enables new ways to enhance properties or even to produce functions not conceivable by other routes. Designing chemical or synthetic biological systems that use coherence optimally is a challenge for future work.

When designing for function, we should address the following questions. (1) Shall we take a modular approach and design building blocks that work using coherence and then assemble them? Will these building blocks perform the desired function or will the desired function emerge collectively only once the units are coupled? (2) How will the system scale? How will the macroscopic function that will probably appear—and be explainable classically—be enabled by coherence at the microscopic level? (3) What sorts of materials will enable scaling?

Highlighting quantum interference effects requires a non-intuitive balance of factors at the molecular scale[87] and suggests that scaling the design to more complex systems has great potential despite its challenges. One of the issues to address is the question of timescales, in particular how long the coherence needs to be sustained (see Box 1) to provide function before the phase information is lost. While the relevant timescale is not always the rate of the dynamical process, it is useful to consider for molecular transport junctions, for instance, how long the electron resides

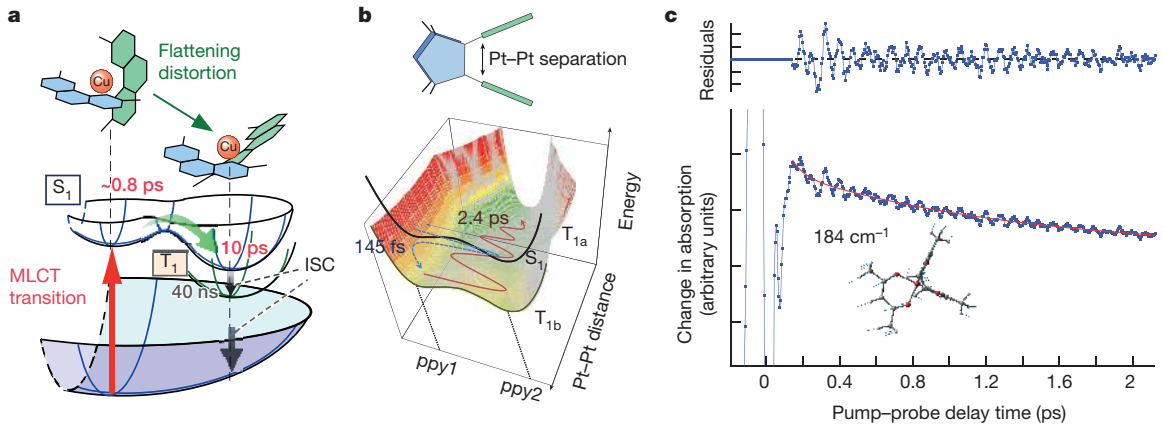

Figure 5 | Coherent motion in transition metal complexes. a, Schematic diagram of the mechanism of the photoinduced structural change of $[Cu(dmphen)_2]^+$ and the concomitant coherent vibrational wavepacket motion. MLCT, metal-to-ligand charge transfer; ISC, intersystem crossing; S_1, first excited singlet electronic state; T_1, first excited triplet electronic state. Image reproduced from ref. 84, American Chemical Society. **b**, Energy relaxation diagram for $[Pt(ppy)(\mu\text{-}tert\text{-}Bu_2pz)]_2$ elucidated from femtosecond pump–probe anisotropy data superimposed on potential energy curves. The colours define contours on the energy axis. Image reproduced from ref. 85, American Chemical Society. **c**, Transient kinetics measured for $Cr(acac)_3$ (inset structure) following excitation into the lowest-energy spin-allowed ligand-field state[86].

on the molecule as it passes from one electrode to another[88]. When the electron tunnels, this so-called contact time is very short (about 1 fs), but it increases markedly in the resonance regime and, in tandem, the scattering becomes inelastic.

Decoherence is not always detrimental—indeed, it can be deployed to achieve function. Recent work, for instance, has predicted that fluctuations can produce coherence that drives the production of mobile carriers in organic solar cells[89]. An example of quantum effects interplaying with kinetics and decoherence is the 'quantum ratchet', or rectifier[78,90,91]. The principle is, essentially, that coherence helps to reduce the efficacy of back-reactions otherwise enabled by the detailed balance condition. The concept is that a fast-forward reaction involves free evolution in the basis of delocalized states, the next-fastest process is decoherence that localizes the product state, and then the even slower back-reaction is suppressed because it is limited to incoherent dynamics. This ensures unidirectional transfer, which causes a rectifier action, and has been suggested to be especially relevant for the FMO complex, which functions as a quantum wire or diode for excitons. A hypothesis for charge separation in conjugated oligomer–fullerene blends is also such an example[92].

Whether coherence can be harnessed in synthetic chemistry is an interesting, and immensely challenging, question. Chemical transformations are often considered based on electronegativity arguments, where reactive groups (electron-rich or -poor) attack molecules, and form new bonds. At first glance, such mechanisms involve multiple electrons in the structure but, in practice, they typically occur as one-electron steps via transition states. Since energetic barriers for making and breaking bonds are high, these reactions proceed relatively slowly. To analyse the timescales and seek opportunities where coherence could be used in optimization, we propose that defining a contact time would be useful, analogous to that described for the molecule transport junctions.

Quantum chemical dynamics calculations have predicted roles for coherence underpinning catalysis, specifically the role of molecules interfacing with a semiconductor[93]. Many important photo-induced reactions require redox steps (for example, water oxidation). The redox flexibility of transition-metal complexes combined with the sensitivity of their geometry to oxidation state presents opportunities for coupling light absorption with multi-electron chemistry. Whether or not multielectron transfers can be achieved coherently is an unanswered question, although one- versus two-electron transfer processes have been studied theoretically[94]. A hint as to the difficulty of the problem is revealed by comparing the energy scales in a molecule of orbital energies (one-particle energies) to the electron correlation corrections for the electronic states, which are much smaller.

As a specific example, consider the Diels–Alder cycloaddition reaction, which cyclizes a diene together with an alkene. Two pathways are conceivable[95]. (1) The reaction pathway happens in two incoherent intermediate steps—the reactants are hinged together, then tethered to complete the cyclization. (2) The pathway forms these partial bonds synchronously, yielding a cyclic intermediate that subsequently relaxes geometrically and electronically to the product. It has been established that the activation barrier for this latter mechanism is lower than the sequential pathway, but only slightly. Ultrafast spectroscopic studies in the gas phase have suggested that both concerted and sequential pathways can be involved[96]. What is not clearly resolved is whether the concerted mechanism can be classed as coherent.

Proton-coupled electron transfer is ubiquitous in biology and is also important for realizing difficult chemical transformations, including production of solar fuels[97,98]. An opportunity for coherence is in the coordination of the electron and proton transfer, where quantum effects are relevant because these are light particles. Evidence suggests they can be concerted[99], but to what extent are they quantum-mechanically coherent? Interestingly, many of the principles discussed in this Review are relevant to the mechanistic details of proton-coupled electron transfer reactions[100].

Open questions and forecast

Coherence and how it affects function are not as mysterious as sometimes perceived. Although so far much of the experimental work has been devoted to demonstrating its existence in specific physical, chemical or biological systems, there are many examples of coherence phenomena, from synthetic chemistry to coherent scattering phenomena to van der Waals forces. These examples illustrate that the use of coherence for function can be practical and is not limited to exotic materials at low temperature.

We suggest that the focus should now shift from confirming the existence of coherence to exploring the connection between coherence and function. This area of investigation will require extensive feedback between theory and experiment, synthesis and measurement, and the development of systematic methods to quantify the influence of coherence in specific processes or devices.

Exploration of function requires controlled perturbation and establishing this essential methodology requires new control mechanisms and clear assessment tools. For instance, the experimental techniques need to measure delocalization of wavefunctions as well as the collapse of delocalized states that will serve to elucidate quantum-ratchet-like effects. Initial steps in this direction have been reported, showing that the ratio of vibronic intensities we described in section 'Vibronic coherence' can

be used to track localization in time by measuring the time-evolving fluorescence spectrum[60].

Attosecond laser sources have already opened up the ability to study coherent electronic motion, such as charge migration and quantum interference between electrons[101,102]. Attosecond lasers may enable studies of electron-nuclear wavepacket motion[103]. Similarly, advances in time-resolved X-ray spectroscopies open up new probes of electronic structure[104,105]. Inspired by coherent multiple scattering and molecular transport junctions, the reactivity of metal centres might be directed or redox chemistry tuned by interference effects to modify the electron density at an active site of a catalyst.

In coherent backscattering, which provides scattering that is twice as bright as diffuse scattering, substantial gains are possible when robust coherence phenomena are exploited. Such gains warrant future research into coherence as a potential force for enhancing function. Although many fundamental problems remain to be investigated, we conclude that the prospects for coherence-enabled function are bright—like Saturn's rings when viewed with zero phase angle.

Received 2 July; accepted 7 December 2016.

1. Wolf, P. E. & Maret, G. Weak localization and coherent backscattering of photons in disordered media. *Phys. Rev. Lett.* **55,** 2696–2699 (1985).
2. Aeschlimann, M. *et al.* Perfect absorption in nanotextured thin films via Anderson-localized photon modes. *Nat. Phys.* **9,** 663–668 (2015).
3. Wiersma, D. The physics and applications of random lasers. *Nat. Phys.* **4,** 359–367 (2008).
4. Cao, H. *et al.* Random laser action in semiconductor powder. *Phys. Rev. Lett.* **82,** 2278–2281 (1999).
5. John, S. Localization of light. *Phys. Today* **44,** 32–40 (1991).
6. Ambrosetti, A., Ferri, N., DiStasio, R. A., Jr & Tkatchenko, A. Wavelike charge density fluctuations and van der Waals interactions at the nanoscale. *Science* **351,** 1171–1176 (2016).
7. Engel, G. S. *et al.* Evidence for wavelike energy transfer through quantum coherence in photosynthetic systems. *Nature* **446,** 782–786 (2007).
Coherence in a photosynthetic protein is detected using two-dimensional electronic spectroscopy.
8. Collini, E. & Scholes, G. D. Coherent intrachain energy migration in a conjugated polymer at room temperature. *Science* **323,** 369–373 (2009).
9. Collini, E. *et al.* Coherently wired light-harvesting in photosynthetic marine algae at ambient temperature. *Nature* **463,** 644–647 (2010).
10. Panitchayangkoon, G. *et al.* Long-lived quantum coherence in photosynthetic complexes at physiological temperature. *Proc. Natl Acad. Sci. USA* **107,** 12766–12770 (2010).
11. Rozzi, C. A. *et al.* Quantum coherence controls the charge separation in a prototypical artificial light-harvesting system. *Nat. Commun.* **4,** 1602 (2013).
12. Walschaers, M., Schlawin, F., Wellens, T. & Buchleitner, A. Quantum transport on disordered and noisy networks: an interplay of structural complexity and uncertainty. *Annu. Rev. Condens. Matter Phys.* **7,** 223–248 (2016).
13. Michler, P. *et al.* Quantum correlation among photons from a single quantum dot at room temperature. *Nature* **406,** 968–970 (2000).
14. Bennett, C. H. & DiVincenzo, D. P. Quantum information and computation. *Nature* **404,** 247–255 (2000).
15. Norbeck, J. & Gallup, G. Valence-bond calculation of the electronic structure of benzene. *J. Am. Chem. Soc.* **96,** 3386–3393 (1974).
16. Naleway, C. A., Curtiss, L. A. & Miller, J. R. Superexchange-pathway model for long-distance electronic couplings. *J. Phys. Chem.* **95,** 8434–8437 (1991).
17. Albinsson, B. & Martensson, J. Long-range electron and excitation energy transfer in donor-bridge-acceptor systems. *J. Photochem. Photobiol. Photochem. Rev.* **9,** 138–155 (2008).
18. Winkler, J. R. & Gray, H. B. Long-range electron tunneling. *J. Am. Chem. Soc.* **136,** 2930–2939 (2014).
19. Zhang, Y., Liu, C., Balaeff, A., Skourtis, S. S. & Beratan, D. N. Biological charge transfer via flickering resonance. *Proc. Natl Acad. Sci. USA* **111,** 10049–10054 (2014).
20. Nitzan, A. & Ratner, M. A. Electron transport in molecular wire junctions. *Science* **300,** 1384–1389 (2003).
21. Aradhya, S. V. & Venkataraman, L. Single-molecule junctions beyond electronic transport. *Nat. Nanotechnol.* **8,** 399–410 (2013).
22. Guédon, C. M. *et al.* Observation of quantum interference in molecular charge transport. *Nat. Nanotechnol.* **7,** 305–309 (2012).
Electrical transport junctions reveal quantum interference through single molecules.
23. Manrique, D. Z. *et al.* A quantum circuit rule for interference effects in single-molecule electrical junctions. *Nat. Commun.* **6,** 6389 (2015).
24. Solomon, G. C., Herrmann, C. & Ratner, M. A. Molecular electronic junction transport: some pathways and some ideas. *Top. Curr. Chem.* **313,** 1–38 (2012).
25. Nitzan, A. Electron transmission through molecules and molecular interfaces. *Annu. Rev. Phys. Chem.* **52,** 681–750 (2001).
26. Valkenier, H. *et al.* Cross-conjugation and quantum interference: a general correlation? *Phys. Chem. Chem. Phys.* **16,** 653–662 (2014).
27. Rebentrost, P., Mohseni, M., Kassal, I., Lloyd, S. & Aspuru-Guzik, A. Environment-assisted quantum transport. *New J. Phys.* **11,** 033003 (2009).
28. Cassette, E., Pensack, R. D., Mahler, B. & Scholes, G. D. Room-temperature exciton coherence and dephasing in two-dimensional nanostructures. *Nat. Commun.* **6,** 6086 (2015).
29. Heller, E. J. A semiclassical way to molecular spectroscopy. *Acc. Chem. Res.* **14,** 368–375 (1981).
30. Berry, H. G., Gabrielse, G. & Livingston, A. E. Measurement of the Stokes parameters of light. *Appl. Opt.* **16,** 3200–3205 (1977).
31. James, D., Kwiat, P., Munro, P. & White, A. Measurement of qubits. *Phys. Rev. A* **64,** 052312 (2001).
32. Lundeen, J. S., Sutherland, B., Patel, A., Stewart, C. & Bamber, C. Direct measurement of the quantum wavefunction. *Nature* **474,** 188–191 (2011).
Weak measurement is used to measure the transverse spatial wavefunction of a single photon.
33. Lundeen, J. S. & Bamber, C. Procedure for direct measurement of general quantum states using weak measurement. *Phys. Rev. Lett.* **108,** 070402 (2012).
34. Spano, F. C. The spectral signatures of Frenkel polarons in H- and J-aggregates. *Acc. Chem. Res.* **43,** 429–439 (2010).
35. Reimers, J. R., McKemmish, L. K., McKenzie, R. H. & Hush, N. S. Non-adiabatic effects in thermochemistry, spectroscopy and kinetics: the general importance of all three Born-Oppenheimer breakdown corrections. *Phys. Chem. Chem. Phys.* **17,** 24641–24665 (2015).
36. Köuppel, H., Domcke, W. & Cederbaum, L. S. Multimode molecular dynamics beyond the Born-Oppenheimer approximation. *Adv. Chem. Phys.* **57,** 59–246 (1984).
37. Schröter, M. *et al.* Exciton–vibrational coupling in the dynamics and spectroscopy of Frenkel excitons in molecular aggregates. *Phys. Rep.* **567,** 1–78 (2015).
38. Christensson, N., Kauffmann, H. F., Pullerits, T. & Mančal, T. Origin of long-lived coherences in light-harvesting complexes. *J. Phys. Chem. B* **116,** 7449–7454 (2012).
39. Barbara, P. F., Walker, G. C. & Smith, T. P. Vibrational modes and the dynamic solvent effect in electron and proton transfer. *Science* **256,** 975–981 (1992).
40. Tiwari, V., Peters, W. K. & Jonas, D. M. Electronic resonance with anticorrelated pigment vibrations drives photosynthetic energy transfer outside the adiabatic framework. *Proc. Natl Acad. Sci. USA* **110,** 1203–1208 (2013).
41. Plenio, M. B., Almeida, J. & Huelga, S. F. Origin of long-lived oscillations in 2D-spectra of a quantum vibronic model: electronic versus vibrational coherence. *J. Chem. Phys.* **139,** 235102 (2013).
42. Novelli, F. *et al.* Vibronic resonances facilitate excited-state coherence in light-harvesting proteins at room temperature. *J. Phys. Chem. Lett.* **6,** 4573–4580 (2015).
43. Fujihashi, Y., Fleming, G. R. & Ishizaki, A. Impact of environmentally induced fluctuations on quantum mechanically mixed electronic and vibrational pigment states in photosynthetic energy transfer and 2D electronic spectra. *J. Chem. Phys.* **142,** 212403 (2015).
44. Chin, A. W. *et al.* The role of non-equilibrium vibrational structures in electronic coherence and recoherence in pigment-protein complexes. *Nat. Phys.* **9,** 113–118 (2012).
45. O'Reilly, E. J. & Olaya-Castro, A. Non-classicality of the molecular vibrations assisting exciton energy transfer at room temperature. *Nat. Commun.* **5,** 3012 (2014).
Theoretical analysis suggests that vibronic coherence can be rigorously quantum mechanical.
46. Romero, E. *et al.* Quantum coherence in photosynthesis for efficient solar-energy conversion. *Nat. Phys.* **10,** 676–682 (2014).
47. Fuller, F. D. *et al.* Vibronic coherence in oxygenic photosynthesis. *Nat. Chem.* **6,** 706–711 (2014).
48. Falke, S. M. *et al.* Coherent ultrafast charge transfer in an organic photovoltaic blend. *Science* **344,** 1001–1005 (2014).
49. Walschaers, M., Diaz, J. F., Mulet, R. & Buchleitner, A. Optimally designed quantum transport across disordered networks. *Phys. Rev. Lett.* **111,** 180601 (2013).
50. Yamagata, H. & Spano, F. C. Vibronic coupling in quantum wires: applications to polydiacetylene. *J. Chem. Phys.* **135,** 054906 (2011).
51. Spano, F. C. & Yamagata, H. Vibronic coupling in J-aggregates and beyond: a direct means of determining the exciton coherence length from the photoluminescence spectrum. *J. Phys. Chem. B* **115,** 5133–5143 (2011).
Theoretical modelling shows how photoluminescence measurements can gauge delocalization of excitons.
52. Dubin, F. *et al.* Macroscopic coherence of a single exciton state in an organic quantum wire. *Nat. Phys.* **2,** 32–35 (2006).
53. Scholes, G. D., Fleming, G. R., Olaya-Castro, A. & van Grondelle, R. Lessons from nature about solar light harvesting. *Nat. Chem.* **3,** 763–774 (2011).
54. Scholes, G. D. & Rumbles, G. Excitons in nanoscale systems. *Nat. Mater.* **5,** 683–696 (2006).
55. Schlau-Cohen, G. S. *et al.* Elucidation of the timescales and origins of quantum electronic coherence in LHCII. *Nat. Chem.* **4,** 389–395 (2012).
56. Brédas, J. L., Sargent, E. H. & Scholes, G. D. Photovoltaic concepts inspired by coherence effects in photosynthetic systems. *Nat. Mater.* **16,** 35–44 (2016).
57. Wu, C., Malinin, S., Tretiak, S. & Chernyak, V. Exciton scattering and localization in branched dendrimeric structures. *Nat. Phys.* **2,** 631–635 (2006).

58. Scholak, T., Mintert, F., Wellens, T. & Buchleitner, A. Transport and entanglement. *Semicond. Semimet.* **83,** 1–38 (2010).
59. Yong, C. *et al.* Ultrafast delocalization of excitation in synthetic light-harvesting nanorings. *Chem. Sci.* **6,** 181–189 (2015).
60. Sung, J., Kim, P., Fimmel, B., Würthner, F. & Kim, D. Direct observation of ultrafast coherent exciton dynamics in helical π-stacks of self-assembled perylene bisimides. *Nat. Commun.* **6,** 8646 (2015).
61. Aggarwal, A. V. *et al.* Fluctuating exciton localization in giant π-conjugated spoked-wheel macrocycles. *Nat. Chem.* **5,** 964–970 (2013).
62. van Oijen, A. M., Ketelaars, M., Kohler, J., Aartsma, T. J. & Schmidt, J. Unraveling the electronic structure of individual photosynthetic pigment-protein complexes. *Science* **285,** 400–402 (1999).
63. Monshouwer, R., Abrahamsson, M., van Mourik, F. & van Grondelle, R. Superradience and exciton delocalization in bacterial photosynthetic light-harvesting systems. *J. Phys. Chem. B* **101,** 7241–7248 (1997).
The shortened radiative rate of fluorescence from a photosynthetic complex shows robust exciton delocalization length.
64. Mirkovic, T. *et al.* Light absorption and energy transfer in the antenna complexes of photosynthetic organisms. *Chem. Rev.* **117,** 249–293 (2016).
65. Scholes, G. D. & Fleming, G. R. On the mechanism of light-harvesting in photosynthetic purple bacteria: B800 to B850 energy transfer. *J. Phys. Chem. B* **104,** 1854–1868 (2000).
A theory explaining how energy transfer is accelerated by exciton states is reported.
66. Sumi, H. Theory on rates of excitation-energy transfer between molecular aggregates through distributed transition dipoles with application to the antenna system in bacterial photosynthesis. *J. Phys. Chem. B* **103,** 252–260 (1999).
A theory explaining how energy transfer is accelerated by exciton states is reported.
67. Huh, J. *et al.* Atomistic study of energy funneling in the light-harvesting complex of green sulfur bacteria. *J. Am. Chem. Soc.* **136,** 2048–2057 (2014).
68. Ishizaki, A. & Fleming, G. R. Unified treatment of quantum coherent and incoherent hopping dynamics in electronic energy transfer: reduced hierarchy equation approach. *J. Chem. Phys.* **130,** 234111 (2009).
69. Lee, M. K., Huo, P. & Coker, D. F. Semiclassical path integral dynamics: photosynthetic energy transfer with realistic environment interactions. *Annu. Rev. Phys. Chem.* **67,** 639–668 (2016).
70. Ishizaki, A. & Fleming, G. R. Quantum coherence in photosynthetic light harvesting. *Annu. Rev. Condens. Matter Phys.* **3,** 333–361 (2012).
71. Chenu, A. & Scholes, G. D. Coherence in energy transfer and photosynthesis. *Annu. Rev. Phys. Chem.* **66,** 69–96 (2015).
72. Ishizaki, A., Calhoun, T. R., Schlau-Cohen, G. S. & Fleming, G. R. Quantum coherence and its interplay with protein environments in photosynthetic electronic energy transfer. *Phys. Chem. Chem. Phys.* **12,** 7319–7337 (2010).
73. Jonas, D. M. Two-dimensional femtosecond spectroscopy. *Annu. Rev. Phys. Chem.* **54,** 425–463 (2003).
74. Mukamel, S. Multidimensional femtosecond correlation spectroscopies of electronic and vibrational excitations. *Annu. Rev. Phys. Chem.* **51,** 691–729 (2000).
75. Mukamel, S. *et al.* Coherent multidimensional optical probes for electron correlations and exciton dynamics: from NMR to X-rays. *Acc. Chem. Res.* **42,** 553–562 (2009).
76. Hayes, D. & Engel, G. S. Extracting the excitonic Hamiltonian of the Fenna-Matthews-Olson complex using three-dimensional third-order electronic spectroscopy. *Biophys. J.* **100,** 2043–2052 (2011).
77. Snaith, H. Perovskites: the emergence of a new era for low-cost, high-efficiency solar cells. *J. Phys. Chem. Lett.* **4,** 3623–3630 (2013).
78. Ishizaki, A. & Fleming, G. R. Theoretical examination of quantum coherence in a photosynthetic system at physiological temperature. *Proc. Natl Acad. Sci. USA* **106,** 17255–17260 (2009).
79. Zhu, X. Y. & Podzorov, V. Charge carriers in hybrid organic-inorganic lead halide perovskites might be protected as large polarons. *J. Phys. Chem. Lett.* **6,** 4758–4761 (2015).
80. Frost, J. M. & Walsh, A. What is moving in hybrid halide perovskite solar cells? *Acc. Chem. Res.* **49,** 528–535 (2016).
81. Zhu, H. *et al.* Screening in crystalline liquids protects energetic carriers in hybrid perovskites. *Science* **353,** 1409–1413 (2016).
82. Liu, C. *et al.* Engineering nanometre-scale coherence in soft matter. *Nat. Chem.* **8,** 941–945 (2016).
83. Bersuker, I. B. Modern aspects of the Jahn-Teller effect theory and applications to molecular problems. *Chem. Rev.* **101,** 1067–1114 (2001).
84. Iwamura, M., Takeuchi, S. & Tahara, T. Ultrafast excited-state dynamics of copper(I) complexes. *Acc. Chem. Res.* **48,** 782–791 (2015).
85. Cho, S. *et al.* Coherence in metal-metal-to-ligand-charge-transfer transitions of a dimetallic complex investigated by ultrafast transient absorption anisotropy. *J. Phys. Chem. A* **115,** 3990–3996 (2011).
86. Schrauben, J., Dillman, K., Beck, W. & McCusker, J. Vibrational coherence in the excited state dynamics of Cr(acac)(3): probing the reaction coordinate for ultrafast intersystem crossing. *Chem. Sci.* **1,** 405–410 (2010).
87. Gorczak, N. *et al.* Computational design of donor-bridge-acceptor systems exhibiting pronounced quantum interference effects. *Phys. Chem. Chem. Phys.* **18,** 6773–6779 (2016).
88. Nitzan, A., Jortner, J., Wilkie, J., Burin, A. & Ratner, M. Tunneling time for electron transfer reactions. *J. Phys. Chem. B* **104,** 5661–5665 (2000).
89. Bittner, E. R. & Silva, C. Noise-induced quantum coherence drives photo-carrier generation dynamics at polymeric semiconductor heterojunctions. *Nat. Commun.* **5,** 3119 (2014).
90. Hoyer, S., Ishizaki, A. & Whaley, K. B. Spatial propagation of excitonic coherence enables ratcheted energy transfer. *Phys. Rev. E* **86,** 041911 (2012).
91. Dittrich, T., Ketzmerick, R., Otto, M. & Schanz, H. Classical and quantum transport in deterministic Hamiltonian ratchets. *Ann. Phys.* **9,** 755–763 (2000).
92. Bakulin, A. A. *et al.* The role of driving energy and delocalized states for charge separation in organic semiconductors. *Science* **335,** 1340–1344 (2012).
93. Akimov, A. V., Asahi, R., Jinnouchi, R. & Prezhdo, O. V. What makes the photocatalytic CO_2 reduction on N-doped Ta_2O_5 efficient: insights from nonadiabatic molecular dynamics. *J. Am. Chem. Soc.* **137,** 11517–11525 (2015).
94. Zusman, L. & Beratan, D. Two-electron transfer reactions in polar solvents. *J. Chem. Phys.* **105,** 165–176 (1996).
95. Houk, K., González, J. & Li, Y. Pericyclic reaction transition states: passions and punctilios, 1935–1995. *Acc. Chem. Res.* **28,** 81–90 (1995).
96. Horn, B., Herek, J. & Zewail, A. Retro-Diels-Alder femtosecond reaction dynamics. *J. Am. Chem. Soc.* **118,** 8755–8756 (1996).
97. Weinberg, D. R. *et al.* Proton-coupled electron transfer. *Chem. Rev.* **112,** 4016–4093 (2012).
98. Huynh, M. H. & Meyer, T. J. Proton-coupled electron transfer. *Chem. Rev.* **107,** 5004–5064 (2007).
99. Rhile, I. J. *et al.* Concerted proton-electron transfer in the oxidation of hydrogen-bonded phenols. *J. Am. Chem. Soc.* **128,** 6075–6088 (2006).
100. Hammes-Schiffer, S. & Soudackov, A. V. Proton-coupled electron transfer in solution, proteins, and electrochemistry. *J. Phys. Chem. B* **112,** 14108–14123 (2008).
101. Calegari, F. *et al.* Charge migration induced by attosecond pulses in bio-relevant molecules. *J. Phys. At. Mol. Opt. Phys.* **49,** 142001 (2016).
102. Hohenleutner, M. *et al.* Real-time observation of interfering crystal electrons in high-harmonic generation. *Nature* **523,** 572–575 (2015).
103. Bredtmann, T., Chelkowski, S. & Bandrauk, A. Monitoring attosecond dynamics of coherent electron-nuclear wave packets by molecular high-order harmonic generation. *Phys. Rev. A* **84,** 021401 (2011).
104. Capano, G. *et al.* Probing wavepacket dynamics using ultrafast x-ray spectroscopy. *J. Phys. At. Mol. Opt. Phys.* **48,** 214001 (2015).
105. Mukamel, S., Healion, D., Zhang, Y. & Biggs, J. D. Multidimensional attosecond resonant X-ray spectroscopy of molecules: lessons from the optical regime. *Annu. Rev. Phys. Chem.* **64,** 101–127 (2013).
106. Rafiq, S. & Scholes, G. D. Slow intramolecular vibrational relaxation leads to long-lived excited-state wavepackets. *J. Phys. Chem. A* **120,** 6792–6799 (2016).
107. Jacobs, K. & Steck, D. A straightforward introduction to continuous quantum measurement. *Contemp. Phys.* **47,** 279–303 (2006).

Acknowledgements We gratefully acknowledge the Division of Chemical Sciences, Geosciences and Biosciences, Office of Basic Energy Sciences of the US Department of Energy. We thank M. Spitler and J. Krause for leading the organization of the Basic Energy Sciences workshop on 'Optimal Coherence in Chemical and Biophysical Dynamics'. G.D.S. thanks E. Sorensen for explaining electrophilic aromatic substitution reactions. We thank E. D. Foszcz for providing Fig. 5c. We thank L. T. Rumbles for improving the manuscript.

Author Contributions L.X.C. proposed the workshop to the Department of Energy Council for Chemical and Biochemical Sciences. G.D.S. and G.R.F. wrote the paper with substantive input from all co-authors. All the authors formulated and discussed the content of the paper and commented on the manuscript.

Author Information Reprints and permissions information is available at www.nature.com/reprints. The authors declare no competing financial interests. Readers are welcome to comment on the online version of the paper. Correspondence and requests for materials should be addressed to G.D.S. (gscholes@princeton.edu) or G.R.F. (GRFleming@lbl.gov).

Reviewer Information *Nature* thanks C. Lienau, A. Troisi and the other anonymous reviewer(s) for their contribution to the peer review of this work.